ResearchGate

See discussions, stats, and author profiles for this publication at: https://www.researchgate.net/publication/256376405

Sequence-specific transitions of the torsion angle gamma change the polar-hydrophobic profile of the DNA grooves...

Article *in* Journal of biomolecular Structure & Dynamics · September 2013

DOI: 10.1080/07391102.2013.830579 · Source: PubMed

CITATIONS
2

READS
46

3 authors, including:

M. Y. Tkachenko
National Academy of Sciences of Ukraine
7 PUBLICATIONS **24** CITATIONS

SEE PROFILE

Anna Shestopalova
Usikov Institute for Radiophysics and Electro...
34 PUBLICATIONS **120** CITATIONS

SEE PROFILE

Some of the authors of this publication are also working on these related projects:

Project

Minor-groove electrostatic potential of free and bound DNA View project

All content following this page was uploaded by Anna Shestopalova on 19 December 2016.

The user has requested enhancement of the downloaded file. All in-text references underlined in blue are added to the original document and are linked to publications on ResearchGate, letting you access and read them immediately.

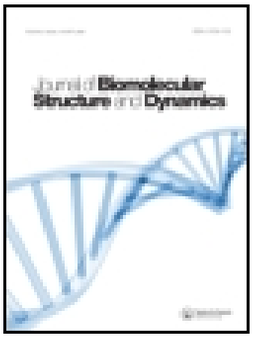

Journal of Biomolecular Structure and Dynamics

ISSN: 0739-1102 (Print) 1538-0254 (Online) Journal homepage: http://www.tandfonline.com/loi/tbsd20

DNA minor groove electrostatic potential: influence of sequence-specific transitions of the torsion angle gamma and deoxyribose conformations

M.Y. Zhitnikova & A.V. Shestopalova

To cite this article: M.Y. Zhitnikova & A.V. Shestopalova (2016): DNA minor groove electrostatic potential: influence of sequence-specific transitions of the torsion angle gamma and deoxyribose conformations, Journal of Biomolecular Structure and Dynamics, DOI: 10.1080/07391102.2016.1255259

To link to this article: http://dx.doi.org/10.1080/07391102.2016.1255259

View supplementary material

Accepted author version posted online: 01 Nov 2016.
Published online: 16 Nov 2016.

Submit your article to this journal

Article views: 15

View related articles

View Crossmark data

Full Terms & Conditions of access and use can be found at
http://www.tandfonline.com/action/journalInformation?journalCode=tbsd20

Download by: [Our Lady of the Lake University], [Mariia Zhitnikova] **Date:** 15 December 2016, At: 13:55

Journal of Biomolecular Structure and Dynamics, 2016
http://dx.doi.org/10.1080/07391102.2016.1255259

DNA minor groove electrostatic potential: influence of sequence-specific transitions of the torsion angle gamma and deoxyribose conformations

M.Y. Zhitnikova* and A.V. Shestopalova

O. Ya. Usikov Institute for Radiophysics and Electronics, National Academy of Sciences of Ukraine, Acad. Proskury Street, 12 Kharkiv 61085, Ukraine

Communicated by Ramaswamy H. Sarma

(*Received 2 July 2016; accepted 24 October 2016*)

The structural adjustments of the sugar-phosphate DNA backbone (switching of the γ angle (O5′–C5′–C4′–C3′) from canonical to alternative conformations and/or C2′-endo → C3′-endo transition of deoxyribose) lead to the sequence-specific changes in accessible surface area of both polar and non-polar atoms of the grooves and the polar/hydrophobic profile of the latter ones. The distribution of the minor groove electrostatic potential is likely to be changing as a result of such conformational rearrangements in sugar-phosphate DNA backbone. Our analysis of the crystal structures of the short free DNA fragments and calculation of their electrostatic potentials allowed us to determine: (1) the number of classical and alternative γ angle conformations in the free B-DNA; (2) changes in the minor groove electrostatic potential, depending on the conformation of the sugar-phosphate DNA backbone; (3) the effect of the DNA sequence on the minor groove electrostatic potential. We have demonstrated that the structural adjustments of the DNA double helix (the conformations of the sugar-phosphate backbone and the minor groove dimensions) induce changes in the distribution of the minor groove electrostatic potential and are sequence-specific. Therefore, these features of the minor groove sizes and distribution of minor groove electrostatic potential can be used as a signal for recognition of the target DNA sequence by protein in the implementation of the indirect readout mechanism.

Keywords: electrostatic potential; DNA conformation; minor groove recognition

Introduction

One of the most important and still unresolved problems of modern molecular biology and biophysics is to understand the nature of molecular recognition, in particular, the specific mechanisms of protein–DNA recognition: how does such large and diverse number of DNA-binding proteins recognize their specific binding sites?

At present, the following conceptions of highly specific protein–DNA recognition are based on two mechanisms of protein-DNA readout: direct and indirect.

Direct readout is recognition of short DNA fragments resulting from formation of the specific hydrogen bonds between protein amino acids and nucleotide functional groups. The basis for this mechanism of recognition is a unique arrangement of the bases atomic groups–donors and acceptors of hydrogen bonds in the major groove of the DNA (Coulocheri, Pigis, Papavassiliou, & Papavassiliou, 2007; Seeman, Rosenberg, & Rich, 1976). In the minor groove, arrangement of donors and acceptors of hydrogen bonds, determined by the base sequence, does not allow to distinguish T/A from A/T and G/C from C/G pairs (Coulocheri et al., 2007).

The second mechanism is indirect readout (Otwinowski et al., 1988; Rohs, West, Liu, & Honig, 2009; Travers, 1989). It is based on the ability of the DNA molecules to sequence specific deformations and conformational transitions, which lead to deviations of DNA structure from the canonical B-DNA double helix. Polymorphism of the double helix and different propensity of specific DNA sequences to structural adjustment are used by proteins to recognize their binding sites. Many proteins combine different mechanisms of readout to achieve greater specificity of protein–DNA recognition (Rohs et al., 2010).

The thousands of available X-ray and NMR structures were analyzed for better understanding of protein-DNA recognition process (Rohs, West, Liu et al., 2009). Recently new, expanded and refined, conceptions of the direct and indirect readout mechanisms were formulated (Rohs, West, Sosinsky et al., 2009). Authors of the review (Rohs et al., 2010) propose to use the more precise terms: ‘base readout’ when protein recognizes a particular base pair, and ‘shape readout’ when protein recognizes a particular DNA shape.

Obviously, local deviation of the DNA double helix conformation leads not only to changes in its shape, but also to changes in the physicochemical properties, particularly at relatively short sequences. One of the most

*Corresponding author. Email: allusio@gmail.com

© 2016 Informa UK Limited, trading as Taylor & Francis Group

important physical parameters of the DNA double helix is the distribution of the electrostatic potential, because DNA is a polyanion with a negative net charge (Cherstvy, 2011; Chin, Sharp, Honig, & Pyle, 1999; Manning, 1978). This negative charge is located on the phosphate groups (Jayaram, Sharp, & Honig, 1989; Pullman & Pullman, 1981; Weiner, Langridge, Blaney, Schaefer, & Kollman, 1989), which contain the bulk of charge, while the deoxyriboses provide an opportunity for hydrophobic interactions in addition to the hydrophobic functional groups of the bases, such as the thymine methyl group.

For an ideal B-DNA helix, negative electrostatic potential of AT-containing sequences in the minor groove is higher than that of GC-containing DNA (Jayaram et al., 1989). This difference is caused by the presence of various electronegative and electropositive atoms in A/T and G/C base pairs. The G/C base pair in the minor groove has a positively charged N_2H_2 group of Guanine. In the AT sequence (A-tract) the negative electrostatic potential of minor groove is affected by negatively charged N3 Adenine atoms, O2 Thymine atoms (Jayaram et al., 1989), and the tendency of A/T pairs to narrow minor groove (Rohs, West, Liu et al., 2009; Rohs, West, Sosinsky et al., 2009; Rohs et al., 2010). So, DNA electrostatic potential correlates with GC content but does not correspond to it exactly and is strongly dependent on both the sequence arrangement and its context, especially flanking regions (Osypov, Krutinin, & Kamzolova, 2010).

For several decades, the complementarity between both the shape and the electrostatic surface potential of the binding partners has been noted (Lavery & Pullman, 1982; Matthew & Ohlendorf, 1985; Weber & Steitz, 1984), but the influence of the structure of DNA on its electrostatic surface potential has only recently been discovered (Rohs et al., 2010; West, Rohs, Mann, & Honig, 2010). Regions with a narrow minor groove are associated with enhanced negative electrostatic potential (Rohs, West, Sosinsky et al., 2009). Decrease in minor groove width leads to phosphates getting closer to each other and, consequently, to the increase in the minor groove negative electrostatic potential (Tullius, 2009). One of the ways of shape readout mechanism realization is 'recognition' of A-tracts by proteins containing Arginine, which have excess positive charge (e.g. HOX group protein (Rohs, West, Liu et al., 2009; Rohs, West, Sosinsky et al., 2009; West et al., 2010)). The study of role of minor groove geometry in the recognition of DNA sequence has shown that HOX group proteins can detect minimal changes in the minor groove geometry and electrostatic potential (Joshi et al., 2007). Hence, shape readout includes any form of structural readout based on global and local DNA shape features, including the stiffness of DNA double helix, conformational flexibility, and shape-dependent electrostatic potential (Harteis & Schneider, 2014; Savelyev, Materese, & Papoian, 2011; Slattery et al., 2014).

In addition to minor groove width, DNA electrostatic potential can be influenced by the distribution of electron density of base pairs 'at the bottom' of the groove, the conformation of the deoxyribose, and the position of the phosphates relative to the boundaries of the grooves (Lavery & Pullman, 1982; Srinivasan et al., 2009).

The formation of many DNA–protein complexes requires the B→A transition of DNA, such as observed in GC-rich stretches of DNA. For example, the bound DNA in the Tc3 transposase-DNA complex has a distinct and extensive electronegative potential patch on the G-side of its A-like major groove (Boschitsch & Fenley, 2011; Harris et al., 2012). The protein Tc3 transposase has several positively charged side chains along one side of the major groove and in the narrow minor groove, forming numerous hydrogen bonds and salt bridges in the grooves (Watkins, van Pouderoven, & Sixma, 2004). Apparently, these unique features of the electrostatic potential around A-DNA are very relevant to biological processes (Harris et al., 2012; Locasale, Napoli, Chen, Berman, & Lawson, 2009). In addition, deoxyribose switching from B- to A-like form contributes to the formation of hydrophobic contacts in the minor groove, increasing the accessible surface area (ASA) of the bases and sugar phosphate backbone atoms (Locasale et al., 2009; Tolstorukov, Jernigan, & Zhurkin, 2004).

An additional mechanism for DNA to adopt a complementary form to its binding partner is through the deviation from the Watson–Crick double helix and the formation of Hoogsteen base pairs (Honig & Rohs, 2011). The different base-pairing geometry affects the shape of the DNA-binding site, its electrostatic potential, and in turn, the strength of DNA–protein interactions (Kitayner et al., 2010).

Analysis of crystallographic structures of protein–DNA complexes shows that the conformational changes of the sugar-phosphate DNA backbone can be used as a mechanism of DNA recognition in the minor groove (Moravek, Neidle, & Schneider, 2002; Tolstorukov et al., 2004; Zhitnikova, Boryskina, & Shestopalova, 2014). For example, the BI and BII conformations of the sugar-phosphate DNA backbone affect the size of the minor groove (Heddi, Abi-Ghanem, Lavigne, & Hartmann, 2010; Moravek et al., 2002; Svozil, Kalina, Omelka, & Schneider, 2008). This influence is the result of correlation that exists between position of phosphate in BII conformation and local parameters of base pairs (Roll and Displacement) (Djuranovic & Hartmann, 2003, 2004; Hartmann, Piazzola, & Lavery, 1993; Winger, Liedl, Pichler, Hallbrucker, & Mayer, 1999). The negative Roll values and displacement of base pairs in the direction towards the major groove is observed in the BII conformations. These structural changes in the sugar-phosphate backbone lead

to changes in the sizes of the grooves: minor groove becomes deeper and wider, and the major groove becomes shallow and narrow (Oguey, Foloppe, & Hartmann, 2010).

The complete results of high-resolution proteins, DNA, and protein–DNA complexes crystal structures provide an opportunity for successful statistical analysis of classical and alternative sugar-phosphate backbone conformations simultaneously with dinucleotide and tetramer sequence effects as a key factor for understanding the influence of conformational fitting on DNA–protein complexation. The results of numerous investigations demonstrate that the analysis of a large set of dinucleotides and tetramers belonging to crystal oligomers (Coulocheri et al., 2007; Locasale et al., 2009; Otwinowski et al., 1988; Rohs, West, Liu et al., 2009; Rohs, West, Sosinsky et al., 2009; Rohs et al., 2010; Tullius, 2009 and references therein) are in agreement with available solution data (Rhodes & Klug, 1981; Rife et al., 1999; Ulyanov & James, 1995; Wynveen, Lee, & Kornyshev, 2008). So one can directly extrapolate the fine structure of a given DNA sequence from a crystal to solution state and crystal structure analysis should be a fruitful method to better understand the conformational peculiarities available to nucleic acids.

Previously, we have shown that the structural adjustment of the sugar-phosphate DNA backbone (switching of the γ angle (O5′–C5′–C4′–C3′) from canonical to alternative conformations and/or C2′-endo → C3′-endo transition of deoxyribose) lead to the sequence-specific changes in ASA of both polar and non-polar atoms of the grooves and the polar/hydrophobic profile of the latter ones (Zhitnikova et al., 2014). Consequently, polarity of the grooves changes: the minor groove becomes more polar and major groove becomes more hydrophobic. The distribution of the minor groove electrostatic potential is likely to be changing as a result of such conformational rearrangements in sugar-phosphate DNA backbone.

To justify the assumption we have analyzed, the available crystal structures of protein–DNA complexes focusing on sequence-specific preferences of γ angle transitions from the canonical *gauche* + to the alternative *gauche*– and *trans* conformations and switching of deoxyribose ring configuration from C2′-endo (B-like) to C3′-endo (A-like) conformation.

As it is known, the free DNA sequences reveal same structural changes as the protein–DNA complexes (Locasale et al., 2009; Oguey et al., 2010). Therefore, studying the conformational features of the free B-DNA is important for understanding the mechanisms of protein–nucleic acid recognition in the early stages of the highly specific protein–DNA complex formation processes.

Our analysis of the crystal structures of the free DNA fragments and calculation of their electrostatic potentials allowed us to determine: (1) the number of classical and alternative γ angle conformations in the free B-DNA; (2) changes in the minor groove electrostatic potential, depending on the conformation of the sugar-phosphate DNA backbone; (3) the effect of the DNA sequence on the minor groove electrostatic potential.

Materials and methods

Data-set of crystallographic structures

The presented analysis was based on the data-set excluded from NDB (Berman et al., 1992; Narayanan et al., 2014). The analyzed database contains 70 crystallographic structures with resolution better than 2 Å (Table 1). All structures contain double-stranded DNA fragments with non-modified bases. In order to avoid end effects all terminal bases were extracted from the analysis. The maximal and minimal lengths of used DNA fragments were 12 base pairs (34 structures) and 6 base pairs (2 structures) respectively. There were oligonucleotides of 11 base pairs (1 structure), 10 base pairs (32 structures), and 9 base pairs (1 structure) in our set of DNA fragments. In total, we analyze 830 nucleotides (or 415 base pairs) including 65.4% of A/T base pairs and 34.6% of G/C base pairs.

All 70 fragments of free B-DNA that we have chosen were divided into groups according to their two central base pairs or steps of nucleotide pairs (step, Table 1 and hereinafter).

From each group, we selected unique hexamers with the same central steps flanked by different steps of nucleotide pairs. We reviewed 23 unique hexamer sequences with 14 of them being represented by only one sequence and the other nine sequences being represented by two or more sequences.

It should be noted that sequences selected for the analysis are palindromic, i.e. they are identical in 5′-3′ direction of the Strand I and 3′-5′ direction of the Strand II.

Calculation of DNA conformational parameters

The values of torsion angle γ (O5′–C5′–C4′–C3′) and sugar phase angle (P) were calculated with 3DNA/CompDNA program (Gorin, Zhurkin, & Olson, 1995; Lu & Olson, 2008).

Values of γ angle were classified according to classical three-fold pattern into: *gauche* + (60° ± 30°), *trans* (180° ± 30°), *gauche* – (300° ± 30°) conformations. The sugar conformations were defined according to values of phase angle P: B-like (C2′-endo or 'South', $90° < p < 220°$) and A-like (C3′-endo or 'North', $-60° < p < 90$).

All complementary pairs of nucleotides were numbered in both directions starting with the central positions ±1, followed by ±2 and ±3 etc.

Table 1. PDB IDs of free B-DNA crystallographic structures selected for the analysis. PDB IDs of crystal structures with plotted distributions of the minor groove electrostatic potential are represented in bold.

Step	Hexamer	NDB (PDB) ID	Step	Hexamer	NDB (PDB) ID
	AACGTT	**5DNB**, **1EN3**, **1EN8**		TTTAAA	**1IKK**, **1SK5**
	AGCGCT	**1EN9**, **1ENE**, **1ZF5**		TATATA	**473D**
	ATCGAT	**1D23**	TA	ATTAAT	**1D49**
CG	GACGTC	**423D**		ACTAGT	**bdj061**
	CTCGAG	**196D**, **251D**		GTTAAC	**1ZF0**
	GTCGAC	**1ZF7**		AGTACT	**1D8G**
	GCCGGC	1ZFB*		AAATTT	**1S2R**, **4AH1**
	TGGCCA	**334D, 126D**		ATATAT	**1D56**, **1D57**
	AAGCTT	**158D**		CAATTG	1JTL*, 432D*, 1Z8 V*, 1S23, **431D**
GC	AGGCCT	**1BD1**	AT		1BNA, **1DOU**, 1EHV, 1ENN, 1FMS, 1FQ2, 1JGR, 1M6F, 1VZK, **1ZFF**, 1ZPH, 2B0 K, 2B3E, 2DYW, 2GVR,
	GAGCTC	**1ZFG**		GAATTC	**3U08**, 2GYX, 2I2I, 355D, 360D, 3U05, 3U0U,
TG	AATGTT	3BSE			428D, 442D, 443D,
GA	AAGAAA	307D			453D, 455D, 463D, 476D, 477D, 4AGZ, 7BNA, 9BNA, 3U2 N, 2QEG

*Structures with positive values of electrostatic potential.

Pair of nucleotides was considered as having an alternative conformation of γ angle if at least one of the nucleotides in any of the complementary chains had an alternative conformation ('switched pair of nucleotide'). Step of nucleotide pair was considered as having alternative conformation of γ angle, if the second nucleotide of the step from 5′-end of any of two strands had an alternative conformation (switched nucleotide pair step).

A-like nucleotides comprised 0.5% of all examined nucleotides. The number of nucleotides containing the *trans*- and *gauche*-conformations of γ angle, amounted to 0.4 and 0.6% of the total number of nucleotides (or 0.7–1.2% of the examined pairs of nucleotides), respectively.

Minor groove width was calculated with 3DNA/CompDNA program (Gorin et al., 1995; Lu & Olson, 2008) based on the algorithm of El Hassan and Calladine (El Hassan & Calladine, 1998).

Calculation of electrostatic potential

The calculation of electrostatic potentials was performed using the software package DelPhi (Li et al., 2012), which was based on the solution of the nonlinear Poisson–Boltzmann equation. All calculations were done at physiological salt concentration of 0.145 M. The charges and atomic radii were taken from the Amber force field (Cornell et al., 1995). The following dielectric parameters were used: internal molecular dielectric constant $\varepsilon = 2$ and the dielectric constant of the surrounding water $\varepsilon = 80$.

Electrostatic potential was calculated at the reference point i located near 'bottom' of minor groove, approximately in the plane of the base pair i (Figure 1).

Reference point i is defined as a geometric center between O4′ atoms of $i + 1$ nucleotide in Strand I (5′-3′ direction) and i-1 nucleotide in Strand II (3′-5′ direction) of DNA double helix. This definition of reference point allows one to estimate the minor groove electrostatic potential for single complementary nucleotide pair (Joshi et al., 2007).

For selected sequences, we plotted the dependence of minor groove electrostatic potential on the position of a particular complementary pair of nucleotides (see Figures 3–6 below).

The hexamers with central AT step (the largest group containing 44 structures) have similar profile of the minor groove electrostatic potential. Therefore, for the analysis of this group, we selected 8 hexamers that have 4 sequences with different nucleotide composition. To analyze the same dependence of GAATTC hexamer (35 structures), we chose 3 structures with minimal, maximal, and intermediate values of the minor groove electrostatic potential.

In some structures, DNA is strongly bent into the major groove and the reference point clashed with amino group of Guanine, causing large positive values of electrostatic potential of the minor groove (Table 1). Sequences which contain pairs of nucleotides with positive values of electrostatic potential were not included in the analysis of minor groove potential sequence specificity, but they were used in statistical analysis. Structures which contain pairs of nucleotides with positive values of electrostatic potential (1JTL, 432D, 1Z8 V, 1ZFB) were not included in the analysis of distribution of hexanucleotide electrostatic potential of minor groove, but they were used in overall statistical analysis.

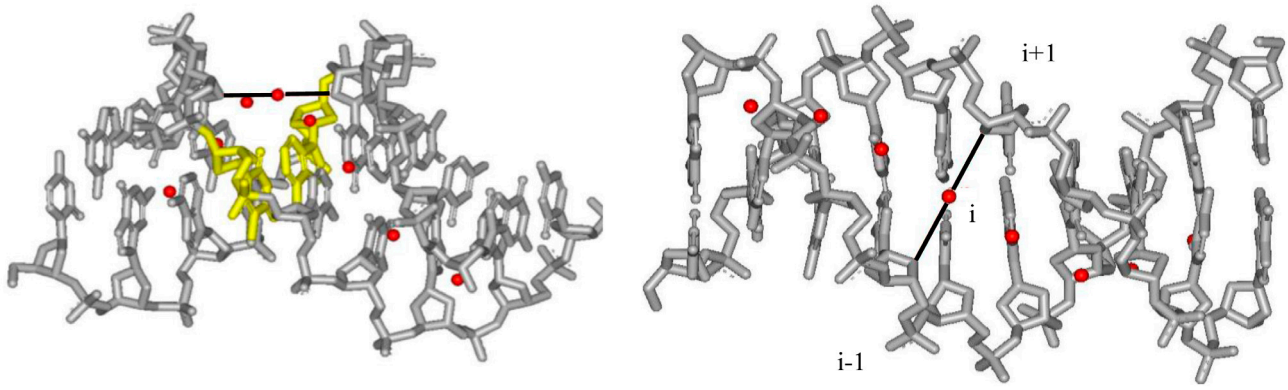

Figure 1. Schematic view of the reference point i, which is defined as geometric center between O4′ atoms of $i-1$ and $i+1$ nucleotides.

Calculation of similarity matrix

To analyze the dependence of the minor groove electrostatic potential shape on the DNA structure and sequence, we calculate similarity matrixes based on Euclidean distance.

Euclidean distance reflects similarity of objects to each other. The greater the distance, the more objects differ. This measure is the geometric distance in the multidimensional space. In our calculations, every curve of the electrostatic potential is represented by a point in a multidimensional space. Its similarity to the other curves is determined as the corresponding distance between two different points. For identical curves, the Euclidean distance is equal to 0.

This approach allowed us to compare the profile of the minor groove electrostatic potential for the same and different sequences within selected groups.

Results

General statistical analysis of the minor groove electrostatic potential distribution

Some facts follow the general analysis of our calculations of minor groove size and its electrostatic potential of all DNA fragments selected for our data-set.

The first is that the electrostatic potential and the width of the minor groove depend on the position of pairs of nucleotides relative to the center of free B-DNA fragment. Negative electrostatic potential at the ends of the short DNA fragments decreases (in absolute value) approximately 2.5 times, wherein the minor groove width increases by 10% (about 1Å) (Figure 2).

This fact is explained by the long-range nature of the electrostatic interaction. Therefore, for analysis of the fragments containing more than 9 complementary pairs of nucleotides, we use the central hexamer only. This length is enough to reduce the influence of the missing phosphate groups on the minor groove electrostatic potential (see Supplemental data for details).

The second fact is that general analysis of the sequence specificity of the minor groove electrostatic potential shows that A/T pairs are characterized by more negative minor groove electrostatic potential than G/C pairs, which is consistent with the literature data (Hud & Plavec, 2003; Jayaram et al., 1989; Rohs et al., 2010).

Electrostatic potential of hexanucleotides with different γ angle conformation

According to our data, the transitions of γ angle from canonical *gauche* + conformation to alternative *trans* conformation, observed only in nucleotide pairs

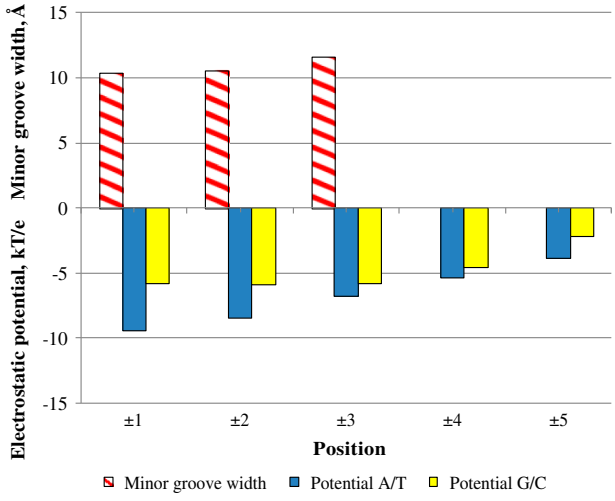

Figure 2. Mean values of electrostatic potential (kT/e) and minor groove width.

containing A/T bases, lead to the increase (in absolute value) in negative electrostatic potential (Table 2).

Previously, we have found that the ASA of polar atoms of sugar-phosphate backbone in minor groove of B-like DNA in complexes with proteins increases from 33.8 to 36.7 Å^2 upon transition of γ angle to *trans* conformation resulting in significant increase in minor groove polarity (Zhitnikova et al., 2014). But it should be noted that such changes in the ASA are not so significant in the free B-DNA fragments. The increased electronegativity of minor groove in sites of localization of such switched pairs of nucleotides is most likely to be explained by the changes in minor groove width. Our calculations of mean values of free B-DNA minor groove width confirmed this assumption. They show that average value of minor groove width is reduced for complementary pairs of nucleotides with *trans* conformation compared to the value of average minor groove width for the ones with classic *gauche* + conformation (Table 2).

Transition into *gauche*-conformation, on the contrary, leads to the decrease in minor groove electronegativity for complementary pair of A/T nucleotides and to a smaller extent for G/C ones. Such effect might be caused by widening of minor groove. Analysis of average values of minor groove width for switched pairs of nucleotides showed that in the *gauche*-conformation, the average minor groove width increases (Table 2). In other words, the reduction of the minor groove electronegativity in the presence of switched *gauche*-nucleotides is caused by the increase in the minor groove width.

Analysis of average values of minor groove width for switched nucleotides showed that in the *gauche*-conformation, the average minor groove width increases (Table 2). In other words, the decrease in the minor groove electronegativity in the presence of switched *gauche*-nucleotides is caused by the widening of minor groove.

The C2′-endo → C3′-endo transition of deoxyribose does not lead to significant changes in the values of the minor groove electrostatic potential neither for A/T or G/C pair of nucleotides; although for pairs of A/T nucleotides with A-like sugar rings, the decrease in the minor groove width was observed in comparison with its size for the B-like conformation of deoxyribose (Table 2).

Distribution of hexanucleotide electrostatic potential

We have analyzed in detail the sequence specificity of the distribution of minor groove electrostatic potential in dependence on the positions of the complementary pairs of nucleotides relative to the center of the DNA fragments. Positions (−1), (1) determine two central pairs of nucleotides. Such dependencies have been plotted for all DNA structures under investigation. We also have calculated and plotted the similarity matrix based on the analysis of the Euclidean distances.

CG step

The analysis of the hexamers with central CG step shows that their minor groove electrostatic potentials are characterized by similar forms which are practically independent of the flanking pairs of nucleotides (Figure 3(a)). The similarity coefficients for these hexamers are ≤3 (Figure 3(b)). So the influence of the nucleotide composition on the values and the distribution of minor groove electrostatic potential for these hexamers are not significant. At the same time, it is known that the xCGx tetramers are sufficiently flexible (Fujii, Kono, Takenaka, Go, & Sarai, 2007). Therefore, according to our data, we

Table 2. The average values of electrostatic potential (kT/e) and width (Å) of minor groove for A/T ad G/C pair of nucleotides with different γ angle conformations: *gauche*+, *gauche*−, *trans* and sugar pucker: B-like or A-like. The average values of minor groove width for nucleotide pair steps in particular positions are given in parentheses.

	A/T		G/C	
Position	Potential	Minor groove width	Potential	Minor groove width
gauche+, B-like				
±1	−9.4	10.4	−5.5	11.2
±2	−8.4	10.3	−5.4	11.7
±3	−6.8	11.2	−5.8	12.7
trans, B-like				
±2	−10.0	9.3 (10.6)	–	–
gauche−, B-like				
±1			−5.1	11.9 (11.7)
±2	−6.6	12.3 (11.25)		
±3			−4.8	14.4 (13.4)
gauche+, A-like				
±2	−8.5	9.6 (10.0)	−5.5	11.2 (11.5)

assume that the effect of flanking pairs of nucleotides on minor groove electrostatic potentials of structures with central CG step is significantly less than their conformational mobility.

The ATCGAT sequence contains the most rigid flanking AT dimer on its ends. It might be the reason for peculiarity of this hexamer in the group. The rigid flanking dimer induces the narrowing of the minor groove up to 9.7 and 9.8 Å at the ends of the fragment (minor groove width in the center fragment is 13.1 Å), and, consequently, the electronegativity of minor groove is increased. The nucleotides with 'switched' γ angle were not found in this group of hexamers.

GC step

The profile of the minor grove electrostatic potential for sequences with rigid central GC step varies slightly (Figure 4), but a bit more than for sequences with the central CG step. According to our data, the average value of electrostatic potential for these sequences is −5.76 ± 1.76 kT/e.

It should be noted that deformability of the xGCx tetranucleotides is the least dependent on the flanking dimers in comparison with deformability of any other tetramers with the central purine–pyrimidine steps (Fujii et al., 2007). Hence, xGCx tetranucleotides are 'rigid' relative to both structure mobility and to variability of the forms of minor groove electrostatic potential.

The maximal similarity (the minimal value of similarity coefficient) for the shapes of minor groove electrostatic potential among the fragments of this group is observed for hexamers AAGCTT and AGGCCT (Figure 4(b)). The minimal similarity (the maximal similarity coefficients, Figure 4(b)) is obtained for the hexamers, which contain switched pairs of nucleotides with alternative γ angle conformations: G**A**GC**T**C and TG**G**CCA (nucleotides with alternative *gauche*-conformation are underlined in particular sequences Figure 4(a)).

The complementary pairs in hexamer G**A**GC**T**C with switched nucleotides in *gauche*- γ angle conformation has more negative minor groove electrostatic potential. Such values of electrostatic potential can be explained by two effects: the changes in (1) the minor groove width and (2) the ASA of polar atoms in sugar-phosphate backbone. The minor groove widths for the steps with switched complementary pair of nucleotides are 12.4 and 12.3 Å (−2 and 2 positions in hexamer G**A**GC**T**C, respectively).

These values are larger than the width of B-DNA minor groove. Therefore, enhancement of electronegativity in this case probably might not be explained by the decrease in minor groove width. We have previously shown (Zhitnikova et al., 2014) that for 'switched' nucleotides with *gauche*-γ angle the ASA of polar atoms of the sugar-phosphate backbone in the minor groove increases by 1.5 times in the protein-nucleic acid complexes. Thus the observed changes of electrostatic potential can be determined by difference in the ASA of polar atoms of sugar-phosphate backbone of nucleotides with switched γ angle.

The TGGCCA hexamers are represented by two structures, which differ in the shape of electrostatic potential (Figure 4(a)). It should be noted that these structures have various conformations of the sugar-phosphate DNA backbone. One of them has switched pair of nucleotides with nucleotide in *gauche*-conformation of γ angle (TG**G**CCA), and the average value of the negative electrostatic potential is greater (in absolute value) in this position (Figure 4(a)).

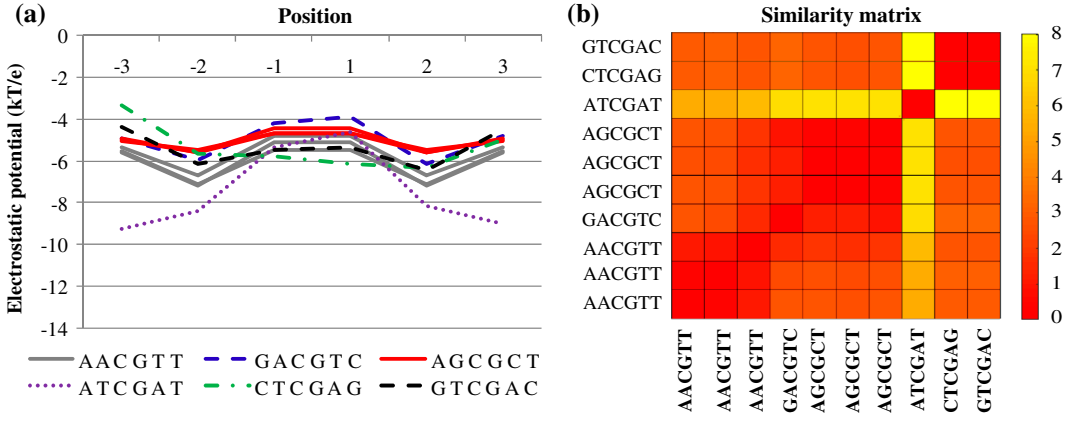

Figure 3. (a) The dependence of the electrostatic potential on the nucleotide position for the sequences with the central CG step, positions (−1), (1) determine two central complementary nucleotide pairs; (b) similarity among the sequences with the central CG step.

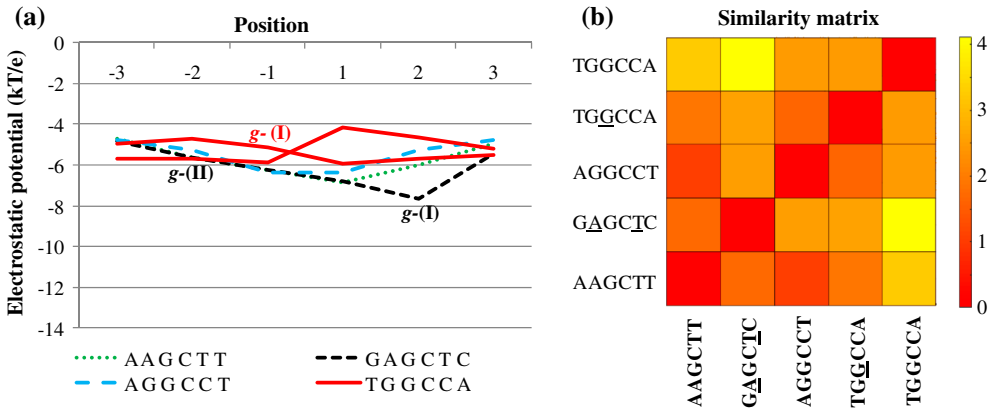

Figure 4. (a) The dependence of the electrostatic potential on the nucleotide position for the sequences with the central GC step, positions (−1), (1) determine two complementary nucleotide pairs, nucleotides with alternative *gauche*-conformation are marked as *g*-(I) in Strand I or *g*-(II) in Strand II; (b) similarity among the sequences with the central GC step, nucleotides with alternative *gauche*-conformation are underlined in particular sequences.

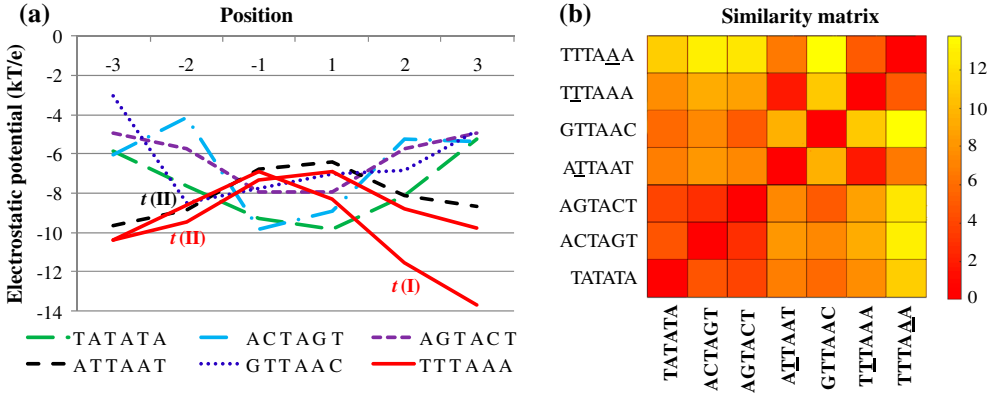

Figure 5. (a) The dependence of the electrostatic potential on the nucleotide position for the sequences with the central TA step, positions (−1), (1) determine two central pairs of nucleotides, nucleotides with alternative *gauche*-conformation are marked as (*t*(I) in Strand I or *t*(II) in Strand II; (b) similarity among the sequences with central TA step, nucleotides with alternative *trans* conformation are underlined in particular sequences.

TA step

The DNA fragments with central TA step are characterized by a significant dispersion of the electrostatic potential values in the minor groove (Figure 5(a)).

What is the reason for such behavior of minor groove electrostatic potential of these sequences? It is known that tetranucleotides xTAx (especially TTAA) were found to be highly deformable (Fujii et al., 2007). According to our calculation, the distribution of the minor groove electrostatic potential of these sequences also significantly depends on the nucleotide composition of the flanking nucleotides.

Switching from the classical *gauche* + γ angle conformation into the alternative *trans* conformation (nucleotides with alternative *trans* conformation are underlined in particular sequences) for complementary pair of nucleotides in A**T**TAAT hexamer and two complementary pairs of nucleotides in T**T**TA**A**A hexamer leads to the substantial distinction in the profile of their minor groove electrostatic potential (Figure 5(a)). The main reason of this difference is the augmentation of the electronegative potential for the complementary pair of nucleotides with 'switched' γ angles for one of the TTTAAA hexamers. The minor groove width of the step with switched pair of nucleotides (position 2, TTTA**A**A) is reduced to 8.5 Å that causes the substantial growth of the minor groove electronegativity (Figure 5(a)).

At the same time A**T**TAAT and T**T**TAAA hexamers with switched pairs of nucleotides both in the position −2 are characterized by the similar profiles (the minimal value of similarity coefficient, Figure 5(b)). They also have similar *minor groove widths* in −2

positions (10.8 and 10.7 Å respectively), which are not substantially different from B-DNA *minor groove width*. Consequently their electronegativity is increased significantly less.

AT step

The minor groove electrostatic potentials of the CAATTG, AAATTT and GAATTC hexamers with the most rigid tetramer AATT (six structures) are characterized by similar forms (Figure 6(a)), but they have some differences in the absolute values (~2 kT/e).

The minor groove electronegativity of such fragments is increased in two central pairs of nucleotides. These data are in agreement with the observation that A-tract narrows minor groove and in this way leads to augmentation of the minor groove electronegative potential (Rohs, West, Liu et al., 2009; Rohs, West, Sosinsky et al., 2009; West et al., 2010). It should be noted that the tetranucleotides with central AT step have sufficiently rigid structures (Nikolov et al., 1996). Perhaps, low deformability of these tetramers defines small variability of the electrostatic potential values independently of the flanking nucleotide pairs.

The ATATAT hexamers with central TATA tetranucleotide (two structures) are characterized by the least similarity of the shape of the minor groove electrostatic potential in comparison with all other DNA fragments in this group (Figure 6(b)). They have an inverse correlation and more positive minor groove electrostatic potential (Figure 6(a)). This effect is explained by the tendency of TATA sequences to widen the minor groove (Nikolov et al., 1996) and, thus, to reduce the electronegative potential.

The γ angle transition into alternative *gauche*-conformation of G/C switched nucleotide pair (nucleotide with alternative *gauche*-conformation is underlined: **G**AATTC, Figure 6(a)), does not lead to noticeable change in the value of the minor groove electrostatic potential in this position.

In addition, it should be noted that some of the PDB structures under investigation have explicitly resolved divalent counterions, which may affect to the DNA conformation and the values of electrostatic potential. Indeed to calculate the minor groove electrostatic potentials and plotted the results as represented on Figures 3–6 we have selected 31 PDB structures. Twenty-three of these structures were obtained with divalent metal ions: Mg^{2+} and Ca^{2+} (1EN3); Mg^{2+} (5DNB, 1EN8, 1EN9, 1ENE, 1D23, 423D, 1IKK, 1D49, 4AH1, 1D57, 431D, 1DOU, 3U08); Ca^{2+} (196D, 1ZF7, 334D, 158D, 1SK5, 1ZF0, 1D8G, 1D56); Ni^{2+} (473D) and 8 structures without such ions (1ZF5, 251D, 126D, 1BD1, 1ZFG, bdj061, 1S2R, 1ZFF).

Consider, for example, hexamer AACGTT from group with central CG step which is represented by three structures (1EN3 with Mg^{2+} and Ca^{2+}; 5DNB, 1EN8 with Mg^{2+}). According to our calculations, the values of their potential and profiles of their distribution in the minor groove are almost identical (Figure 3). Hexamer AGCGCT is also represented by three structures, two of which contained Mg^{2+} (1EN9, 1ENE), and one is obtained without such ion (1ZF5). According to our calculations, the values of their potential and the shape of their distribution in the minor groove are also almost identical (Figure 3). In this group of hexamers, the maximum difference in potential values and their distribution in the minor groove are observed for hexamer ATCGAT with Mg^{2+} (1D23).

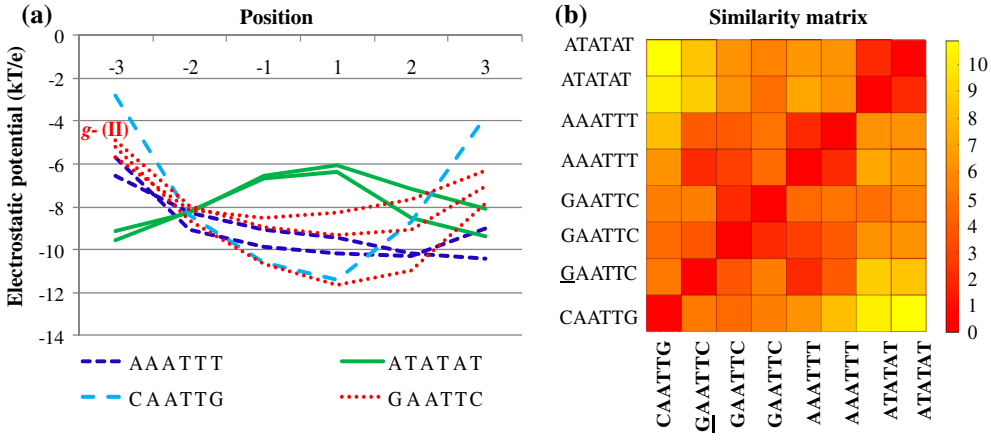

Figure 6. (a) The dependence of the electrostatic potential on the nucleotide position for the sequences with the central AT step, positions (−1), (1) determine two central pairs of nucleotides, nucleotide with alternative *gauche*-conformation is marked as *g*-(II) in Strand II; (b) similarity among the sequences with central AT step, nucleotide with alternative *gauche*-conformation is underlined in particular sequence.

All these facts, in our opinion, allow one to assert that the presence of divalent ions does not explain the observed changes in potential values and in their profile. So it is not necessary to take into account the presence of divalent ions in calculations of electrostatic potentials and their potential influence for the value and profile of electrostatic potential in the minor groove.

Sequence specificity of γ angle transitions

Sequence analysis of short DNA fragments shows that all complementary pairs of nucleotides with alternative γ angle conformations are present in three groups of hexamers under investigation. The *gauche*-conformation is observed in the groups with central GC (Figure 4(a)) and AT (Figure 6(a)) dimers. The *trans* conformation of γ angle is found in the group with hexamers containing central TA step (Figure 5(a)). This fact is in agreement with our data (Zhitnikova et al., 2014). It should be noted that the nucleotides with *gauche*-conformation of γ angle are observed in the hexamers with rigid central xGCx tetranucleotides which are characterized by insignificant dispersion of minor groove electrostatic potentials.

Complex of exonuclease ExoX with two DNA fragments

We have considered the complex of DNA with ExoX exonuclease as an example of existence of the correlation between γ angle conformation, minor groove width, and distribution of electrostatic potential of short DNA fragments.

The exonucleases play an essential role in DNA repair mechanisms. Their function is to remove damaged nucleotides from the 3′ end of the DNA or intact nucleotides in the recombination process (Burdett, Baitinger, Viswanathan, Lovett, & Modrich, 2001; Dermic, 2006; Viswanathan, Burdett, Baitinger, Modrich, & Lovett, 2001; Wang et al., 2013). Endonuclease ExoX belongs to the DnaQ family which is one of the largest superfamilies of 3′-5′ exonucleases. The ExoX exonuclease is one of the several redundant exonucleases involved in the mismatch repair system, UV repair, homologous recombination, and stabilization of the tandem repeats in *E. coli* (Viswanathan et al., 2001).

The fragments of DNA in the complexes with ExoX exonuclease use both Watson–Crick base pairs (PDB 4FZX, conserved DNA with 3′ overhanging dsDNA) and non-Watson-Crick base pairs (PDB 4FZZ, mismatched DNA with 3′ recessed mismatch-containing dsDNA) (Wang et al., 2013).

The first step of the ExoX-DNA complex formation is the ‘capture’ of the DNA fragment by means of the interaction between protein surface and sugar-phosphate backbone of the DNA target site. Formation of such contacts prevents protein ‘slipping off’ the binding sites on DNA before reaction of phosphodiester bond cleavage starts. The contacts also help to keep the DNA chain in the correct position and orientation. Then exonuclease ‘cuts’ phosphodiester bond with subsequent removal of nucleotides.

According to Wang and co-authors (Wang et al., 2013) the protein-binding site contains Lysine, Tyrosine, and Asparagine amino acids in both ExoX–DNA complexes (Lys111, Tyr112 and Asn114: PDB 4FZX, for conserved DNA, and PDB 4FZZ, for mismatched DNA) interacting with sugar-phosphate DNA backbone. Residues Lys101 and Arg104 form specific positively charged binding site with AT step of DNA strand complementary to substrate (Wang et al., 2013).

Our calculations of the electrostatic potential have shown that mismatched DNA in complex with ExoX has more narrow minor groove and enhanced negative electrostatic potential at AT step in comparison with conserved DNA (Table 3) and interacts with Lys101 and Arg104 of ExoX (Figure 7(a)).

The conformation of the mismatched DNA fragment (PDB ID 4FZZ) is also significantly different from the conformation of conserved DNA fragment (PDB ID 4FZX). In the 4FZZ complex Adenine which interacted with Arg104 (A1) has a value of γ angle close to such in *gauche*-conformation (Table. 3).

According to our data (Zhitnikova et al., 2014), such γ angle switching provides maximal value of ASA of O3′ atom in the minor groove. The local rearrangement of the sugar-phosphate DNA backbone creates conditions for formation of the hydrogen bond between O3′ atom of nucleotide containing Adenine A1 and Arg104 (Table 3, Figure 7(b)).

In the complex of ExoX exonuclease with conserved DNA (4FZX) the conformation of γ angle of nucleotide containing Adenine A1 is close to the *trans* conformation (Table. 3). In this situation only electrostatic interaction is possible in the minor groove between DNA fragment and protein.

The distance between the interacting atoms O3′ … HNH is about 3.4 Å (Figure 7(b)) that is larger than the optimal distance between the donor and acceptor groups required to form the hydrogen bond. So the observed structural changes in the mismatched and conserved DNA sugar-phosphate backbone in the complexes are in agreement with the concept of the higher specificity of ExoX exonuclease to mismatched DNA, which is important to increase the efficiency of non-replicative synthesis (Wang et al., 2013).

Table 3. Structural parameters and values of minor groove electrostatic potential (kT/e) for 5′-GGATCC-3′ sequence of conserved DNA (PDB ID 4FZX) and mismatched DNA (PDB ID 4FZZ). The γ angle conformation is shown in parentheses.

	Strand I	−3G	−2G	−1A	1T	2C	3C
Sequence	Strand II	−3C	−2C	−1T	1A[a]	2G	3G
				4FZX			
angle γ	Strand I	33.1 (*g*+)	36.3 (*g*+)	37 (*g*+)	11.2 (~*g*+)	31.7 (*g*+)	15 (~*g*+)[b]
angle γ	Strand II	−11.6 (~*g*–)	−131.6 (~*t*)	18.3 (~*g*+)	125.2 (~*t*)[b]	−172.4 (*t*)[b]	42 (*g*+)
Electrostatic potential		−4.9	−5.7	−6.2	−5.9	−3.8	−3.5
Minor groove width		12.6		12.9	13.0	13.4	–[c]
				4FZZ			
angle γ	Strand I	157.5 (*t*)[b]	162.2 (*t*)[b]	–132.2 (~*t*)	25.4 (~*g*+)	–109 (~g–)	131.1 (~*t*)[b]
angle γ	Strand II	7.2 (~*g*+)	–25.6 (~*g*–)	–90.8 (~*g*–)	–107.1 (~*g*–)	31.4 (*g*+)	49.8 (*g*+)
Electrostatic potential		−3.4	−5.3	−7.4	−6.9	−4.2	−3.5
Minor groove width		13.4	12.1	12.3	12.2	14.0	

[a]Adenine interacting with Arg104.
[b]Nucleotide with A-like sugar pucker.
[c]4FZX and 4FZZ fragments have different amount of nucleotides after 5′-GGATCC-3′ hexamer, so there is no value of minor groove width for CC step of 4FZX structure.

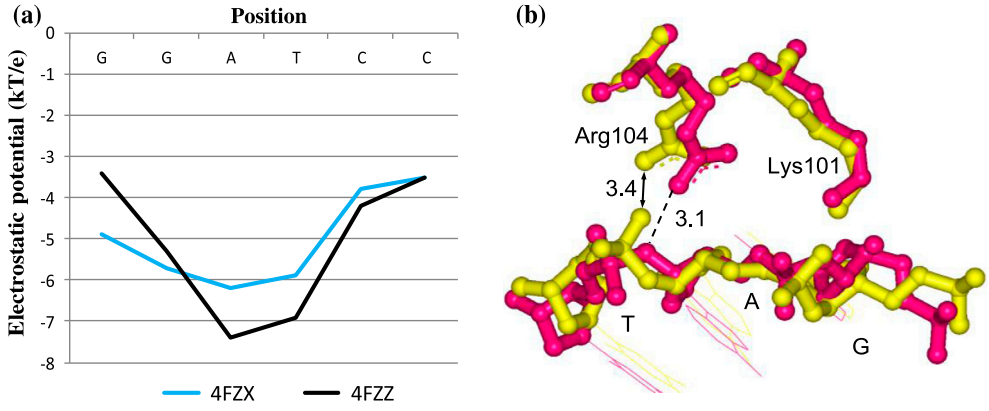

Figure 7. Complexes of ExoX exonuclease with two DNA fragments: (a) the distribution of the minor groove electrostatic potential for the binding site (5′-GGATCC-3′) of 4FZX and 4FZZ structures; (b) contacts between Lys101 and Arg104 with sugar-phosphate DNA backbone of specific binding site with central AT step. The structure of conserved (4FZX) and mismatched (4FZZ) complex are highlighted in yellow and pink colors respectively. The hydrogen bond between O3′ atom of nucleotide containing Adenine and H atom of the amino group NH_2 of Arg104 ($r_{O3' \ldots HNH}$ = 3.1 Å) is shown by the dotted line.

Conclusions

The results of the crystallographic analysis of free DNA structures allows us to determine the existence of the correlations between DNA sequence, structural conformation of the sugar-phosphate backbone, minor groove width and distribution of the minor groove electrostatic potential.

In the present investigation, we confirm our earlier results which determined the sequence-specificity of the γ angle transitions (Zhitnikova et al., 2014). We have found that the *gauche*-conformation is observed in hexamers with central GC step while the *trans* conformation of γ angle is observed in hexamers containing central TA step.

We also determined that the γ angle transitions affect minor groove size and electrostatic potential.

Transition of γ angle into *trans* conformation leads to narrowing of the minor groove that, in its turn, causes the increase of negative electrostatic potential. On the contrary, switching to alternative *gauche*- γ angle conformation induces the decrease of negative electrostatic potential for both A/T and G/C complementary pairs of nucleotides. These changes can be explained by the increase of the minor groove width in sites with switched *gauche*-complementary pairs of nucleotides.

Transition of γ angle from classical *gauche* + conformation into alternative *trans* conformation in hexamers with central TA step results in substantially different forms of distribution of minor groove electrostatic potential. The main reason is as follows: the narrowing of the minor groove in the sites of the switched complementary pairs of nucleotides induces the local increase in the minor groove electronegativity.

In hexamers with central GC step transition to the alternate *gauche*-conformation of γ angle also leads to the increase in minor groove electronegativity for

hexamer GAGCTC. However, the augmentation of negative electrostatic potential in this case might not be explained by the decrease in minor groove width, and the observed growth of the absolute value of electrostatic potential can be determined by difference in the ASA of polar atoms of sugar-phosphate backbone of nucleotide with switched γ angle.

It should be noted that the most flexible sequences with central pyrimidine-purine steps are characterized by different forms of distribution of minor groove electrostatic potential. The hexamers with central TA step are characterized by a significant diversity of the profiles of the electrostatic potential, while the same profiles for sequences with central CG step are remarkably similar. Apparently, the distribution of the minor groove electrostatic potential of hexamers with central TA step is more influenced by flanking nucleotide pairs, whereas hexamers with central CG step are less sensitive to the nucleotide composition of the neighboring pairs.

Thus, our data confirm an important role of the structural reconstruction of the sugar-phosphate DNA backbone in the mechanisms of indirect protein–nucleic acid recognition. We have demonstrated that the structural adjustments of the DNA double helix (the conformations of the sugar-phosphate backbone and the minor groove dimensions) induce changes in the distribution of the minor groove electrostatic potential and are sequence-specific. Therefore, these features of the minor groove sizes and distribution of minor groove electrostatic potential can be used as a signal for recognition of the target DNA sequence by protein in the implementation of the indirect readout mechanism.

Abbreviations

DNA	Deoxyribonucleic acid
A	Adenine
G	Guanine
C	Cytosine
T	Thymine
HOX	Homeobox
ASA	Accessible surface area
NMR	Nuclear magnetic resonance
NDB	Nucleic Acid Data Bank
PDB ID	Protein Data Bank identifier
ExoX	Exonuclease X
UV	Ultraviolet
dsDNA	double-stranded DNA
Lys	Lysine
Tyr	Tyrosine
Asn	Asparagine
Arg	Arginine

Disclosure statement

No potential conflict of interest was reported by the authors.

Funding

This work was supported by NAS of Ukraine [grant number 0111U010475] [Project MODEL-2, 2012–2016].

Supplemental material

The supplementary material for this article is available online at http://dx.doi.org/10.1080/07391102.2016.1255259

References

Berman, H. M., Olson, W. K., Beveridge, D. L., Westbrook, J., Gelbin, A., Demeny, T., … Schneider, B. (1992). The nucleic acid database: A comprehensive relational database of three-dimensional structures of nucleic acids. *Biophysical Journal, 63*, 751–759. doi:10.1016/S0006-3495(92)81649-1

Boschitsch, A. H., & Fenley, M. O. (2011). A fast and robust Poisson–Boltzmann solver based on adaptive cartesian grids. *Journal of Chemical Theory and Computation, 7*, 1524–1540. doi:10.1021/ct1006983

Burdett, V., Baitinger, C., Viswanathan, M., Lovett, S. T., & Modrich, P. (2001). In vivo requirement for RecJ, ExoVII, ExoI, and ExoX in methyl-directed mismatch repair. *Proceedings of the National Academy of Sciences, 98*, 6765–6770. doi:10.1073/pnas.121183298

Cherstvy, A. G. (2011). Electrostatic interactions in biological DNA-related systems. *Physical Chemistry Chemical Physics, 13*, 9942–9968. doi:10.1039/c0cp02796k

Chin, K., Sharp, K. A., Honig, B., & Pyle, A. M. (1999). Calculating the electrostatic properties of RNA provides new insights into molecular interactions and function. *Nature Structural Biology, 6*, 1055–1061. doi:10.1038/14940

Cornell, W. D., Cieplak, P., Bayly, C. I., Gould, I. R., Merz, K. M., Ferguson, D. M., Jr., … Kollman, P. A. (1995). A second generation force field for the simulation of proteins. Nucleic acids, and organic molecules. *Journal of the American Chemical Society, 117*, 5179–5197. doi:10.1021/ja955032e

Coulocheri, S. A., Pigis, D. G., Papavassiliou, K. A., & Papavassiliou, A. G. (2007). Hydrogen bonds in protein–DNA complexes: Where geometry meets plasticity. *Biochimie, 89*, 1291–1303. doi:10.1016/j.biochi.2007.07.020

Dermic, D. (2006). Functions of multiple exonucleases are essential for cell viability, DNA repair and homologous recombination in recD mutants of Eschirichia coli. *Genetics, 172*, 2057–2069. doi:10.1534/genetics.105.052076

Djuranovic, D., & Hartmann, B. (2003). Conformational characteristics and correlations in crystal structures of nucleic acid oligonucleotides: Evidence for sub-states. *Journal of Biomolecular Structure and Dynamics, 20*, 771–788. doi:10.1080/07391102.2003.10506894

Djuranovic, D., & Hartmann, B. (2004). DNA fine structure and dynamics in crystals and in solution: The impact of BI/BII backbone conformations. *Biopolymers, 73*, 356–368. doi:10.1002/bip.10528

El Hassan, M. A., & Calladine, C. R. (1998). Two distinct modes of protein-induced bending in DNA. *Journal of Molecular Biology, 282*, 331–343. doi:10.1006/jmbi.1998.1994

Fujii, S., Kono, H., Takenaka, S., Go, N., & Sarai, A. (2007). Sequence-dependent DNA deformability studied using molecular dynamics simulations. *Nucleic Acids Research, 35*, 6063–6074. doi:10.1093/nar/gkm627

Gorin, A. A., Zhurkin, V. B., & Olson, W. K. (1995). B-DNA twisting correlates with base-pair morphology. *Journal of Molecular Biology, 247*, 34–48. PMID:7897660.

Harris, R. C., Mackoy, T., Dantas Machado, A., Xu, D., Rohs, R., & Fenley, M. O. (2012). Opposites attract: Shape and electrostatic complementarity in protein-DNA complexes. *Innovations in Biomolecular Modeling and Simulations, 2*, 53–80. doi: 10.1039/9781849735056-00053

Harteis, S., & Schneider, S. (2014). Making the bend: DNA tertiary structure and protein-DNA interactions. *International Journal of Molecular Sciences, 15*, 12335–12363. doi:10.3390/ijms150712335

Hartmann, B., Piazzola, D., & Lavery, R. (1993). BI-BII transitions in B-DNA. *Nucleic Acids Research, 21*, 561–568. doi:10.1093/nar/21.3.561

Heddi, B., Abi-Ghanem, J., Lavigne, M., & Hartmann, B. (2010). Sequence-dependent DNA flexibility mediates DNase I cleavage. *Journal of Molecular Biology, 395*, 123–133. doi:10.1016/j.jmb.2009.10.023

Honig, B., & Rohs, R. (2011). Biophysics: Flipping Watson and Crick. *Nature, 470*, 472–473. doi:10.1038/470472a

Hud, N. V., & Plavec, J. (2003). A unified model for the origin of DNA sequence-directed curvature. *Biopolymers, 69*, 144–158. doi:10.1002/bip.10364

Jayaram, B., Sharp, K. A., & Honig, B. (1989). The electrostatic potential of B-DNA. *Biopolymers, 28*, 975–993. doi:10.1002/bip.360280506

Joshi, R., Passner, J. M., Rohs, R., Jain, R., Sosinsky, A., Crickmore, M. A., … Mann, R. S. (2007). Functional specificity of a Hox protein mediated by the recognition of minor groove structure. *Cell, 131*, 530–543. doi:10.1016/j.cell.2007.09.024

Kitayner, M., Rozenberg, H., Rohs, R., Suad, O., Rabinovich, D., Honig, B., & Shakked, Z. (2010). Diversity in DNA recognition by p53 revealed by crystal structures with Hoogsteen base pairs. *Nature Structural & Molecular Biology, 17*, 423–429. doi:10.1038/nsmb.1800

Lavery, R., & Pullman, B. (1982). The electrostatic field of DNA: The role of the nucleic acid conformation. *Nucleic Acids Research, 10*, 4383–4395. doi:10.1093/nar/10.14.4383

Li, L., Li, C., Sarkar, S., Zhang, J., Witham, S., Zhang, Z., … Wang, L. (2012). DelPhi: A comprehensive suite for DelPhi software and associated resources. *BMC Biophysics, 5*(1), 1–9. doi:10.1186/2046-1682-5-9

Locasale, J. W., Napoli, A. A., Chen, S., Berman, H. M., & Lawson, C. L. (2009). Signatures of protein-DNA recognition in free DNA binding sites. *Journal of Molecular Biology, 386*, 1054–1065. doi:10.1016/j.jmb.2009.01.007

Lu, X. J., & Olson, W. K. (2008). 3DNA: A versatile, integrated software system for the analysis, rebuilding, and visualization of three-dimensional nucleic-acid structures. *Nature Protocols, 3*, 1213–1227. doi:10.1038/nprot.2008.14

Manning, G. S. (1978). The molecular theory of polyelectrolyte solutions with applications to the electrostatic properties of polynucleotides. *Quarterly Reviews of Biophysics, 11*, 179–246. doi:10.1017/S0033583500002031

Matthew, J. B., & Ohlendorf, D. H. (1985). Electrostatic deformation of DNA by a DNA-binding protein. *The Journal of Biological Chemistry, 260*, 5860–5862. Retrieved from http://www.jbc.org/content/260/10/5860.long

Moravek, Z., Neidle, S., & Schneider, B. (2002). Protein and drug interactions in the minor groove of DNA. *Nucleic Acids Research, 30*, 1182–1191. doi:10.1093/nar/30.5.1182

Narayanan, B., Westbrook, J., Ghosh, S., Petrov, A. I., Sweeney, B., Zirbel, C. L., … Berman, H. M. (2014). The nucleic acid database: New features and capabilities. *Nucleic Acids Research, 42*, D114–D122. doi:10.1093/nar/gkt980

Nikolov, D. B., Chen, H., Halay, E. D., Hoffman, A., Roeder, R. G., & Burley, S. K. (1996). Crystal structure of a human TATA box-binding protein/TATA element complex. *Proceedings of the National Academy of Sciences, 93*, 4862–4867. Retrieved from http://www.ncbi.nlm.nih.gov/pmc/articles/PMC39370/pdf/pnas01511-0352.pdf

Oguey, C., Foloppe, N., & Hartmann, B. (2010). Understanding the sequence-dependence of DNA groove dimensions: Implications for DNA interactions. *PLoS ONE, 5*, e15931. doi:10.1371/journal.pone.0015931

Osypov, A. A., Krutinin, G. G., & Kamzolova, S. G. (2010). DEPPDB–DNA electrostatic potential properties database: Electrostatic properties of genome DNA. *Journal of Bioinformatics and Computational Biology, 10*, 1–19. doi:10.1142/S0219720010004811

Otwinowski, Z., Schevitz, R. W., Zhang, R. G., Lawson, C. L., Joachimiak, A., Marmorstein, R. Q., … Sigler, P. B. (1988). Crystal structure of trp represser/operator complex at atomic resolution. *Nature, 335*, 321–329. doi:10.1038/335321a0

Pullman, A., & Pullman, B. (1981). Molecular electrostatic potential of the nucleic acids. *Quarterly Reviews of Biophysics, 14*, 289–380. doi:10.1017/S0033583500002341

Rhodes, D., & Klug, A. (1981). Sequence-dependent helical periodicity of DNA. *Nature, 292*, 378–380. doi:10.1038/292378a0

Rife, J. P., Stallings, S. C., Correll, C. C., Dallas, A., Steitz, T. A., & Moore, P. B. (1999). Comparison of the crystal and solution structures of two RNA oligonucleotides. *Biophysical Journal, 76*, 65–75. doi:10.1016/S0006-3495(99)77178-X

Rohs, R., Jin, X., West, S. M., Joshi, R., Honig, B., & Mann, R. S. (2010). Origins of specificity in protein-DNA recognition. *Annual Review of Biochemistry, 79*, 233–269. doi:10.1146/annurev-biochem-060408-091030

Rohs, R., West, S. M., Liu, P., & Honig, B. (2009). Nuance in the double-helix and its role in protein-DNA recognition. *Current Opinion in Structural Biology, 19*, 171–177. doi:10.1016/j.sbi.2009.03.002

Rohs, R., West, S. M., Sosinsky, A., Liu, P., Mann, R. S., & Honig, B. (2009). The role of DNA shape in protein-DNA recognition. *Nature, 461*, 1248–1253. doi:10.1038/nature08473

Savelyev, A., Materese, C. K., & Papoian, G. A. (2011). Is DNA's rigidity dominated by electrostatic or nonelectrostatic interactions? *Journal of the American Chemical Society, 133*, 19290–19293. doi:10.1021/ja207984z

Seeman, N. C., Rosenberg, J. M., & Rich, A. (1976). Sequence-specific recognition of double helical nucleic acids by proteins. *Proceedings of the National Academy of Sciences, 73*, 804–808. Retrieved from http://www.pnas.org/content/73/3/804.full.pdf

Slattery, M., Zhou, T., Yang, L., Dantas Machado, A. C., Gordân, R., & Rohs, R. (2014). Absence of a simple code: How transcription factors read the genome. *Trends in Biochemical Sciences, 39*, 381–399. doi:10.1016/j.tibs.2014.07.002

Srinivasan, A. R., Sauers, R. R., Fenley, M. O., Boschitsch, A. H., Matsumoto, A., Colasanti, A. V., & Olson, W. K. (2009). Properties of the nucleic-acid bases in free and Watson-Crick hydrogen-bonded states: Computational insights into the sequence-dependent features of double-helical DNA. *Biophysical Reviews, 1*, 13–20. doi:10.1007/s12551-008-0003-2

Svozil, D., Kalina, J., Omelka, M., & Schneider, B. (2008). DNA conformations and their sequence preferences. *Nucleic Acids Research, 36*, 3690–3706. doi:10.1093/nar/gkn260

Tolstorukov, M. Y., Jernigan, R. L., & Zhurkin, V. B. (2004). Protein-DNA hydrophobic recognition in the minor groove is facilitated by sugar switching. *Journal of Molecular Biology, 337*, 65–76. doi:10.1016/j.jmb.2004.01.011

Travers, A. A. (1989). DNA conformation and protein binding. *Annual Review of Biochemistry, 58*, 427–452. doi:10.1146/annurev.bi.58.070189.002235

Tullius, T. (2009). Structural biology: DNA binding shapes up. *Nature, 461*, 1225–1226. doi:10.1038/4611225a

Ulyanov, N. B., & James, T. L. (1995). Statistical analysis of DNA duplex structural features. *Methods in Enzymology, 261*, 90–120. doi:10.1016/S0076-6879(95)61006-5

Viswanathan, M., Burdett, V., Baitinger, C., Modrich, P., & Lovett, S. T. (2001). Redundant exonuclease involvement in Escherichia coli methyl-directed mismatch repair. *Journal of Biological Chemistry, 276*, 31053–31058. doi:10.1074/jbc.M105481200

Wang, T., Sun, H. L., Cheng, F., Zhang, X. E., Bi, L., & Jiang, T. (2013). Recognition and processing of double-stranded DNA by ExoX, a distributive 3'-5' exonuclease. *Nucleic Acids Research, 41*, 7556–7565. doi:10.1093/nar/gkt495

Watkins, S., van Pouderoven, G., & Sixma, T. K. (2004). Structural analysis of the bipartite DNA-binding domain of Tc3 transposase bound to transposon DNA. *Nucleic Acids Research, 32*, 4306–4312. doi:10.1093/nar/gkh770

Weber, I. T., & Steitz, T. A. (1984). Model of specific complex between catabolite gene activator protein and B-DNA suggested by electrostatic complementarity. *Proceedings of the National Academy of Sciences, 81*, 3973–3977. Retrieved from http://www.pnas.org/content/81/13/3973.long

Weiner, P. K., Langridge, R., Blaney, J. M., Schaefer, R., & Kollman, P. A. (1989). Electrostatic potential molecular surfaces. *Proceedings of the National Academy of Sciences of the USA, 79*, 3754–3758. Retrieved from http://www.pnas.org/content/79/12/3754.full.pdf

West, S. M., Rohs, R., Mann, R. S., & Honig, B. (2010). Electrostatic interactions between arginines and the minor groove in the nucleosome. *Journal of Biomolecular Structure and Dynamics, 27*, 861–866. doi:10.1080/07391102.2010.10508587

Winger, R. H., Liedl, K. R., Pichler, A., Hallbrucker, A., & Mayer, E. (1999). Helix morphology changes in B-DNA induced by spontaneous B I ⇌B II Substate Interconversion. *Journal of Biomolecular Structure and Dynamics, 17*, 223–235. Retrieved from http://www.ncbi.nlm.nih.gov/pubmed/10563572

Wynveen, A., Lee, D. J., & Kornyshev, A. A. (2008). Helical coherence of DNA in crystals and solution. *Nucleic Acids Research, 36*, 5540–5551. doi:10.1093/nar/gkh514

Zhitnikova, M. Y., Boryskina, O. P., & Shestopalova, A. V. (2014). Sequence-specific transitions of the torsion angle gamma change the polar-hydrophobic profile of the DNA grooves: implication for indirect protein-DNA recognition. *Journal of Biomolecular Structure and Dynamics, 32*, 1670–1685. doi:10.1080/07391102.2013.830579

View publication stats